Morphologic Changes in the Lamina Cribrosa Upon Intraocular Pressure Lowering in Patients With Normal Tension Glaucoma

Jeong-Ah Kim,[1] Seung Hyen Lee,[2] Dong Hwan Son,[3] Tae-Woo Kim,[4] Eun Ji Lee,[4] Michaël J. A. Girard,[5,6] and Jean Martial Mari[7]

[1]Department of Ophthalmology, Kangwon National University School of Medicine, Chuncheon, South Korea
[2]Department of Ophthalmology, Nowon Eulji Medical Center, Eulji University College of Medicine, Seoul, South Korea
[3]Department of Ophthalmology, Hallym University College of Medicine, Chuncheon Sacred Heart Hospital, Chuncheon, Korea
[4]Department of Ophthalmology, Seoul National University College of Medicine, Seoul National University Bundang Hospital, Seongnam, Korea
[5]Department of Biomedical Engineering, National University of Singapore, Singapore
[6]Singapore Eye Research Institute, Singapore National Eye Centre, Singapore
[7]Université de la Polynésie française, Tahiti, French Polynesia

Correspondence: Tae-Woo Kim, Department of Ophthalmology, Seoul National University Bundang Hospital, 82, Gumi-ro, 173 Beon-gil, Bundang-gu, Seongnam, Gyeonggi-do 463–707, Korea; twkim7@snu.ac.kr.

Received: August 4, 2021
Accepted: January 14, 2022
Published: February 11, 2022

Citation: Kim JA, Lee SH, Son DH, et al. Morphologic changes in the lamina cribrosa upon intraocular pressure lowering in patients with normal tension glaucoma. *Invest Ophthalmol Vis Sci.* 2022;63(2):23. https://doi.org/10.1167/iovs.63.2.23

Purpose. The purpose of this study was to investigate whether the lamina cribrosa (LC) curve changes in response to intraocular pressure (IOP) reduction following administration of topical ocular hypotensive eye drops in eyes with normal tension glaucoma (NTG).

Methods. Ninety-three eyes of 93 patients with treatment naïve NTG at initial examination and with ≥20% reduction from baseline IOP following administration of topical ocular hypotensive eye drops were included. Serial horizontal B-scan images of the optic nerve head (ONH) were obtained from each eye using enhanced depth imaging spectral domain optical coherence tomography (OCT) before and 1 year after IOP-lowering treatment. The LC curvature in each eye was assessed by measuring the LC curvature index (LCCI) in horizontal OCT B-scan images obtained at three (superior, central, and inferior) locations spaced equidistantly across the vertical optic disc diameter before and after IOP-lowering treatment. We evaluated the OCT detectible change in the LC curvature based on the interval change of LCCI to exceed the intersession standard deviation of 1.96 times and factors associated with the magnitude of the LCCI change in the eyes showing significant LC change.

Results. IOP decreased from 15.7 ± 2.5 mm Hg at baseline to 11.2 ± 1.7 mm Hg after topical glaucoma medication. Among the 93 subjects, 62 (66.7%) eyes showed the significant reduction of the LCCI (interssetional change over 1.5) after the treatment; greater interssessional change of the LCCI after IOP reduction was associated with younger age ($P = 0.020$) and larger baseline LCCI ($P < 0.001$).

Conclusions. The OCT detectible changes in LC curvature occurred in response to a modest decrease in the IOP in the naïve NTG eyes. The therapeutic benefit of these changes need to be assessed in longitudinal studies.

Keywords: normal tension glaucoma, lamina cribrosa curvature, intraocular pressure reduction, hysteresis of lamina cribrosa, lamina cribrosa

Like primary open angle glaucoma, normal-tension glaucoma (NTG) is a multifactorial optic neuropathy characterized by progressive loss of retinal ganglion cells (RGCs) and their axons, leading to irreversible visual field damage in eyes with an intraocular pressure (IOP) within the statistically normal range. Because IOP is within the normal range in NTG, factors other than IOP-related stress are thought to play a more important role in NTG than in high tension glaucoma. However, considering that IOP is significantly higher in eyes with NTG than in eyes of healthy subjects[1] and that IOP reduction favorably alters the course of visual field progression in patients with NTG,[2] IOP-related stress is also thought to be involved in NTG. Nonetheless, the precise mechanism by which IOP-related stress is involved in the pathogenesis of optic nerve damage in NTG remains unknown.

Mechanical theory indicates that elevated IOP induces deformation of the lamina cribrosa (LC; e.g. displacement of LC insertion,[3,4] posterior bowing,[5,6] and remodeling of connective tissue by reactive astrocytes[7–9]). LC changes

Investigative Ophthalmology & Visual Science

promote damage to axons and their cell bodies by various mechanisms, including blocking axonal transport and diminishing the diffusion of nutrients from the capillaries inside the laminar beams to the adjacent axons.[10] Results of recent studies have suggested that LC strain is likely involved not only in eyes with high tension glaucoma but also in eyes with NTG.[11–13] Evaluation of patients with NTG with unilateral damage has shown that the LC is more deformed in glaucomatous than in fellow healthy eyes.[11] In addition, the LC is more deformed in eyes with NTG than in eyes with nonglaucomatous optic neuropathy, despite having similar IOP and axonal damage.[12,13]

It is unclear, however, whether a posteriorly curved LC in patients with NTG is an innate feature or the result of IOP-induced stress. Thus, it would be of interest to investigate whether LC morphology changes after IOP lowering in patients with NTG. If a posteriorly curved LC results from IOP-induced stress, then the LC will likely be less curved when the IOP is decreased by treatment, as shown in eyes with high tension glaucoma. The present study therefore investigated whether the LC curve in eyes with NTG is altered by IOP lowering treatment with topical ocular hypotensive eye drops.

Methods

This prospective study involved patients with NTG enrolled in the ongoing Investigating Glaucoma Progression Study (IGPS),[14,15] a prospective clinical trial approved by the Institutional Review Board of Seoul National University Bundang Hospital (SNUBH). Written informed consent was obtained from all study participants. The protocol of the present study adhered to the tenets of the Declaration of Helsinki and was approved by the institutional review board of SNUBH.

Study Subjects

All subjects underwent comprehensive ophthalmic examinations, including measurements of best-corrected visual acuity (BCVA); Goldmann applanation tonometry; refraction tests; slit-lamp biomicroscopy; gonioscopy; stereo disc photography; red-free fundus photography (EOS D60 digital camera; Canon, Utsunomiya, Japan); measurements of corneal curvature (KR-1800; Topcon), central corneal thickness (Orbscan II; Bausch & Lomb Surgical, Rochester, NY, USA), and axial length (AXL; IOLMaster version 5; Carl Zeiss Meditec, Dublin, CA, USA); spectral-domain OCT (SD-OCT) scanning of the circumpapillary retinal nerve fiber layer (RNFL); and horizontal B-scan images of the optic nerve head (ONH) using enhanced-depth imaging (EDI) mode with high speed setting (Spectralis; Heidelberg Engineering, Heidelberg, Germany), and standard automated perimetry (Humphrey Field Analyzer II 750, 24-2 Swedish interactive threshold algorithm; Carl Zeiss Meditec).

Systemic blood pressure (BP) was measured by sphygmomanometry with the patient in an upright sitting position after a 10-minute rest period. Mean arterial pressure (MAP) was calculated as MAP = 1/3 systolic BP + 2/3 diastolic BP.

The IGPS excluded subjects with a history of intraocular surgery other than cataract extraction and glaucoma surgery, any intraocular disease (e.g. diabetic retinopathy or retinal vein occlusion) or any neurologic disease (e.g. stroke or brain tumor) that could cause visual field (VF) loss; and subjects with BCVAs worse than 20/40.

All patients included in the IGPS were followed up every 3 to 6 months by regular slit-lamp examinations using a 78-diopter lens or stereo disc photography. Circumpapillary RNFL thickness was measured by SD-OCT scanning at intervals ranging from 6 to 12 months.

NTG was diagnosed based on the presence of glaucomatous optic nerve damage (i.e. notching, neuroretinal rim thinning, and RNFL defect on the stereo disc and red-free photography) with corresponding VF defect, an open angle on gonioscopy, and an IOP ≤21 mm Hg on multiple measurements made on the same day or over a few days before starting IOP-lowering medication. Glaucomatous VF defect was defined as VF (1) outside normal limits on glaucoma hemifield tests; or (2) three abnormal points with a probability $P < 5\%$ of being normal and one point with a $P < 1\%$ by pattern deviation; or (3) a pattern standard deviation with $P < 5\%$ if the VF was otherwise normal, as confirmed in 2 consecutive tests. The VF results were deemed reliable when fixation losses were <20% and the false-positive and false-negative rates were each <25%.

Patients were included in the present study if they were newly diagnosed with NTG at initial examination and were then treated with topical ocular hypotensive eyedrops alone. ONH B-scan images were obtained in all enrolled patients before and after IOP lowering treatment (between 12 and 24 months after confirming a ≥20% reduction from baseline IOP). The IOP measurements using Goldmann applanation tonometry were also recorded at follow-up visits.

Baseline IOP was measured diurnally every 2 hours from 9:00 AM to 5:00 PM (5 measurements) on the same day or on different days, prior to administration of IOP-lowering medications, with the average of these 5 measurements defined as the baseline IOP. The ONH was imaged by SD-OCT using the EDI technique on the same day that baseline IOP was measured. The IOP*b* and IOP*f* were defined as the IOPs measured at baseline and follow-up optic disc scanning, respectively.

Patients showing a <20% decrease in IOP*f* relative to IOP*b* were excluded, as were patients with a documented history of poor adherence or inability to follow through with topical ocular hypotensive eye drops. Patients were also excluded if they had a spherical equivalent <–6.0 D or >+3.0 D; a cylinder correction of <–3.0 D or >+3.0 D, a tilted disc (i.e. a tilt ratio between the longest and shortest diameters of the optic disc of >1.3)[16,17]; or a torted disc (i.e. a >15 degree torsion angle deviation of the long axis of the optic disc from the vertical meridian).[17,18] The measurements of the optic disc tilt and torsion were based on two-dimensional fundus photographs and not on based OCT based measurements as in previous studies.[19,20] Eyes were also excluded if good-quality images (i.e. quality score >15) could not be obtained in more than five sections. If the quality score did not reach 15, the image-acquisition process automatically stopped, or images of the respective sections were not obtained. Only acceptable scans with good-quality images that present clear delineation of the anterior border of the LC within the range of Bruch's membrane (BM) opening (BMO) width were included in measurements of LCCI.

EDI-OCT of the Optic Nerve Head and Adaptive Compensation

LC curvature was assessed using the horizontal B-scan images obtained using the EDI technique of the SD-OCT

Investigative Ophthalmology & Visual Science

system with high speed settings.[21] Prior to disc scanning, the corneal curvature of each eye was entered into the Spectralis OCT system to avoid potential magnification errors. The optic disc was imaged through undilated pupils using a rectangle subtending 10 degrees × 15 degrees of the optic disc. This rectangle was scanned with approximately 75 B-scan section images that were separated by 30 to 34 µm (the distance between the scan lines was determined automatically). Approximately 42 SD-OCT frames were obtained for each section. This protocol provided the best trade-off between image quality and patient cooperation.[22]

To enhance the visibility of the anterior LC surface, all disc scan images were post-processed using adaptive compensation.[23–25]

Measurement of LC Depth and Curvature

The LCD and LCCI were measured at three (superior, central, and inferior) locations equidistant across the vertical optic disc diameter on post-processed horizontal B-scan images, as in our previous study.[26] These three B-scan lines were defined as planes 1 to 3 (superior to inferior regions, Fig. 1A).

Because a bowtie-shaped central ridge is present at or near the mid-horizontal LC,[27] the LC usually has a W-shape in vertical scans, whereas varying in radial scans along the meridians. Therefore, it is difficult to assess the LC configuration using a simple parameter, such as LCCI in vertical or oblique scans. In contrast, LC has a relatively regular configuration in the horizontal plane, having a flat or U-shaped appearance differing in regional steepness.[28–30] Therefore, we assessed the LCD and LCCI on horizontal B-scan images of the ONH (Fig. 1B).

The LCD was defined as the distance between the level of the BMO and the maximally depressed point of the anterior LC surface. A line connecting the temporal and nasal BMO points was drawn on each B-scan image, and the LCD was measured perpendicular to this line toward the maximally depressed LC point (Fig. 1C). The distance between the temporal and nasal BMO points was defined as the BMO width.

The LC curvature was assessed by measuring the LCCI. The method used to calculate LCCI has been described previously.[26,29,31–33] In brief, LCCI was determined by measuring the width of the LC curve reference line (LCCW) and the LC curve depth (LCCD). The LCCW was defined as the width of the line connecting the two points on the anterior LC surface that met the lines drawn from each BM termination point perpendicular to the line connecting these BMO points. The maximum depth from the LC curve reference line to the anterior LC surface was defined as the LCCD (Fig. 1D). The LCCI was calculated as (LCCD/LCCW) × 100. Because the curvature is normalized relative to the LC width, it describes the shape of the LC independent of the actual size of the ONH. Only the LC within the BMO was considered because the LC was often not clearly visible outside the BMO. In eyes with LC defects, the LCCI and LCD were measured using a presumed anterior LC surface that best fit the curvature of the remaining part of the LC or excluded the area of the LC defect. An LC defect was defined as an anterior laminar surface irregularity that violates the smooth curvilinear U- or W-shaped contour with a diameter greater than 100 µm and a depth greater than 30 µm in cross-sectional EDI OCT images.[34,35]

Measurements were made by two experienced observers (J.A.K. and E.J.L.), masked to the clinical information of participants, using a manual caliper tool in Amira software (version 5.2.2; Visage Imaging, Berlin, Germany). If the anterior LC surface was not visualized clearly, measurements were made on an adjacent horizontal EDI OCT scan, located 30 to 34 µm from the original scan. If the anterior LC surface could not be visualized, even on the adjacent scans, the eye was excluded.

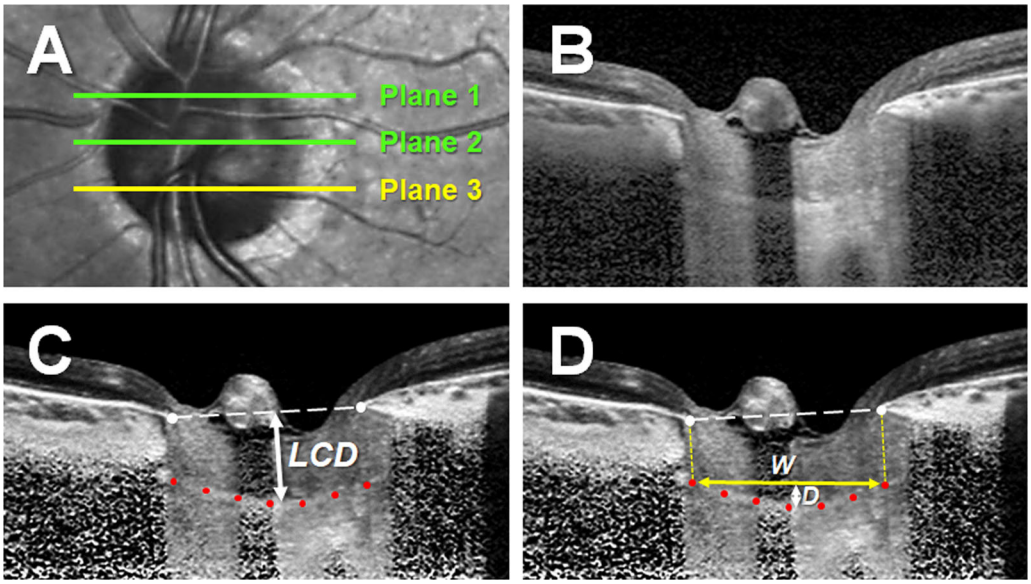

Figure 1. Measurements of LCD and LCCI. (**A**) Infrared fundus image of an optic nerve head with lines indicating the locations of the three horizontal B-scan images. (**B**) B-scan image corresponding to plane 3 in **A**. (**C, D**) Same B-scan images as in **B**, post-processed by adaptive compensation. **C** The LCD was defined as the maximum vertical distance from the BMO reference line (*dashed line*) to the anterior LC surface (*double-headed arrow*). **D** LCCI was measured by dividing the LC curve depth (*D*) within the BMO by the width of the anterior LC surface reference line (*W*), and multiplying the ratio by 100. LCD = lamina cribrosa depth; LCCI = lamina cribrosa curve index; BMO = Bruch's membrane opening.

Investigative Ophthalmology & Visual Science

The average LCD and LCCI were defined as the means of the measurements taken at three points along the LC.

For follow-up measurements, the sets of B-scans were selected to correspond to those selected for the baseline measurements. The correspondences of the selected B-scans between images obtained before and after treatment were confirmed using en face images and the low reflective shadows within the LC shown in B-scan images.[36]

The mean of the measurements made by the two observers was used for analysis.

Measurement of the Peripapillary Choroidal Thickness Using EDI SD-OCT

A 360-degree 3.5-mm diameter peripapillary circle scan centered on the optic disc was performed for RNFL assessment using the EDI technique of the Spectralis OCT (software version 1.6.4.0; Heidelberg Engineering, Heidelberg, Germany).[37] Using the manual segmentation function built into the Heidelberg Eye Explorer software,[38] the posterior edge of the RPE and the sclerochoroidal interface were delineated to represent the inner and outer boundaries of the choroid, respectively. Choroidal thickness was automatically generated in corresponding sectors by the RNFL thickness algorithm function. Two experienced observers (J.A.K. and E.J.L.), masked to the clinical information of the study subjects, measured the peripapillary choroidal thickness, with the mean of the measurements used for analysis.

Statistical Analysis

Data were expressed as mean ± SD except where otherwise indicated. The interobserver agreement for measuring LCD and LCCI was evaluated by calculating the 95% Bland-Altman limits of agreement. The pre- and post-treatment IOPs, LCD, and LCCI were compared using paired *t*-tests. The false discovery rate was controlled for using the Benjamini–Hochberg method.[39]

The intersession variability of the LCD and LCCI was determined from measurements of a separate population of 30 patients with stable NTG who received treatment and had an IOP <15 mm Hg with IOP fluctuations ≤2 mm Hg during the 12 months of follow-up. Each scan was repeated on a different day within a 1-week period, and the 95% intraclass correlation coefficients (ICCs) and intersession SDs were calculated. A statistically significant change (OCT detectible change) was defined as an intersession SD of 1.96 times because it corresponds to the 95% confidence interval for the true value of the measurement.[40] Based on the reversal of LC curvature, subjects were divided into two groups using an LCCI cutoff value of the OCT detectible change. Group 1, showed no significant change in LC curvature, whereas group 2 showed a significant reversal of LC curvature.

Between group differences in numerical and categorical variables were compared using independent-samples *t*-tests and chi-square tests, respectively. Regression analysis was used to determine the factors associated with the changes in the LCD and LCCI in group 2. Variables with *P* values < 0.10 on univariate analysis were included in the multivariate analysis and stepwise backward elimination was utilized to obtain the final multivariable model.

For all analyses, parametric or nonparametric tests were utilized based on the normality of the data. All statistical analyses were performed using SPSS Statistics 22.0 software (IBM, Armonk, NY, USA). Probability values of $P < 0.05$ were considered statistically significant.

Results

Baseline Characteristics

This study initially included 143 patients diagnosed with treatment naïve NTG at initial examination. Of these, 31 patients were excluded due to insufficient IOP lowering or documented poor adherence, thus failing to meet the study inclusion criteria. In addition, 19 subjects were excluded because of poor image quality of their SD-OCT disc scans. The study cohort consisted of 93 eyes of 93 patients. The anterior LC surface was discernible in most of the baseline and follow-up B-scans.

All 93 patients had been newly diagnosed with NTG and treated with topical ocular hypotensive eye drops alone. The clinical characteristics of study participants are shown in Table 1. The 93 patients included 50 (53.8%) men and 43 (46.2%) women, of mean age 59.2 ± 10.2 years. Their baseline IOP was 16.5 ± 2.1 mm Hg, refractive error (spherical equivalent) was −0.62 ± 1.95 diopters, AXL was 23.92 ± 0.99 mm, global RNFL thickness was 76.6 ± 15.5 µm, and VF mean deviation was −6.13 ± 6.84 dB. The baseline LCD was 532.2 ± 132.0 µm (range = 308.7 to 945.3 µm) and the baseline LCCI was 9.07 ± 2.06 (range = 4.27 to 12.97).

Changes in LC Depth and LC Curvature With IOP Reduction

The 95% Bland-Altman limits of agreement between the measurements from the two glaucoma specialists were −24.1 to 21.3 µm for the LCD and −0.82 to 0.95 for the LCCI.

Table 1. Baseline Characteristics of the Study Subjects ($N = 93$)

Variables	Mean ± Standard Deviation
Clinical characteristics	
Age, years	59.2 ± 10.2
Female gender, *n* (%)	43 (46.2)
Diabetes mellitus, *n* (%)	10 (10.8)
Hypertension, *n* (%)	23 (24.7)
Family history of glaucoma, *n* (%)	7 (7.5)
Cold extremities, *n* (%)	22 (23.7)
Migraine, *n*	59.2 ± 10.2
Ocular characteristics	
IOP at baseline, mm Hg	15.7 ± 2.5
Spherical equivalent, D	−0.62 ± 1.95
Central corneal thickness, µm	548.0 ± 32.1
Axial length, mm	23.92 ± 0.99
Global RNFL thickness, µm	76.6 ± 15.5
Visual field MD, dB	−6.13 ± 6.84
Visual field PSD, dB	5.57 ± 4.05
Average BMO width, µm	1397.3 ± 140.7
Average LCD, µm	532.2 ± 132.0
Average LCCI	9.13 ± 2.05
Peripapillary choroidal thickness	164.4 ± 60.6

IOP, intraocular pressure; D, diopter; AXL, axial length; RNFL, retinal nerve fiber layer; MD, mean deviation; dB, decibel; PSD, pattern standard deviation; BMO, Bruch's membrane opening; LCD, lamina cribrosa depth; LCCI, lamina cribrosa curvature index.

Data are presented as mean ± standard deviation or *n* (%).

Investigative Ophthalmology & Visual Science

At the time of post-treatment OCT scan, the mean number of medications taken by each patient was 1.4 ± 0.6. The mean reduction from baseline in IOP was 4.6 ± 1.6 mm Hg (range = 2.0 to 9.0 mm Hg), corresponding to a mean percent reduction of 28.6 ± 7.15 (range = 20% to 50%). The mean reduction from baseline in LCD was 9.13 ± 2.05 µm (range = −25.33 to 92.0 µm) and the mean reduction in LCCI was 2.12 ± 0.72 (range = 0.08 to 4.53).

The intersession reproducibilities based on the LCD and LCCI measurements of 30 patients with stable NTG were excellent, with an ICC for LCD of 0.996 (range = 0.995–0.997) and an ICC for LCCI of 0.946 (range = 0.930–0.959); 1.96 times the intersession SDs were 23.40 µm for LCD and 1.50 for LCCI. Based on these values, 20 (21.5%) eyes showed a significant decrease in LCD and 62 (66.7%) eyes showed a significant decrease in LCCI, with 14 (15.5%) showing significant decreases in both.

Clinical and Ocular Characteristics Relative to Reversal of LC Curvature

Based on the reversal of LC curvature, subjects were divided into two groups using an LCCI cutoff value of 1.50, corresponding to an intersession SD of 1.96 times in 30 patients with stable NTG in the present study. Group 1, consisting of 31 patients, showed no significant change in LC curvature, whereas group 2, consisting of 62 patients, showed a significant reversal of LC curvature (Fig. 2). There were no differences between these two groups in baseline IOP (P = 0.111), corneal thickness (P = 0.946), AXL (P = 0.301), RNFL thickness (P = 0.270), mean deviation of visual field test (P = 0.061), average BMO width (P = 0.348), or reduction in IOP (P = 0.581). At baseline, however, patients in group 1 were significantly older (P = 0.015), and had lower systemic systolic and diastolic BP (P < 0.010 each), a smaller LCCI (P < 0.001), and thinner peripapillary choroid (P = 0.030) than patients in group 2 (Table 2).

Factors Associated With the Reduction of LC Curvature in the Group 2

The factors affecting the reduction of LCCI were determined by linear regression analysis. Univariate analysis showed that younger age at baseline (P = 0.018) and larger LCCI (P < 0.001) were significantly associated with reduction in LCCI. Multivariate analysis also showed that younger age at baseline (P = 0.020) and larger baseline LCCI (P < 0.001) were statistically significant independent factors associated with the magnitude of LCCI reduction (Table 3, Fig. 3).

Representative Case

Figure 4 shows a patient with NTG with reductions in LCD and LC curvature after IOP-lowering treatment.

Discussion

The present study demonstrated that the LC became less curved in about two thirds of eyes with NTG after topical ocular hypotensive medication. The magnitude of LC change was associated with age and baseline LCCI. Patients who showed no detectable LC change were older and had a relatively flat baseline LC, lower ocular perfusion pressure (OPP), and thinner peripapillary choroid than patients with detectable LC change. To our knowledge, this is the first study to document the morphologic changes in the LC after IOP lowering treatment in patients with NTG.

Reversal of LC curvature was greater in younger than in older patients with NTG, consistent with findings in patients with high tension glaucoma.[31,36] With aging, the constituents of the LC undergo various changes, such as having more collagen,[41] smaller pores,[42] alterations in laminar beam thickness,[43] and thicker laminar astrocyte basement membrane. These age-related changes may render the LC stiffer and less responsive to IOP lowering. The decreased flexibility of the LC with age[44–50] may be related to the higher risk of glaucoma progression in elderly subjects. Restoration of a deformed LC is less likely in older subjects, despite IOP reduction, thereby potentially exerting compressive stress continuously on the RGC axon or capillaries inside the LC.

Although the reduction of IOP reduced the LCCI, the magnitude of the LC change was not linearly correlated with the extent of IOP reduction in the current study. This is contrasted to our previous study,[31,36] which reported positive correlation between the mangitue of IOP reduction and the amount of LC curve reduction. We consider that this

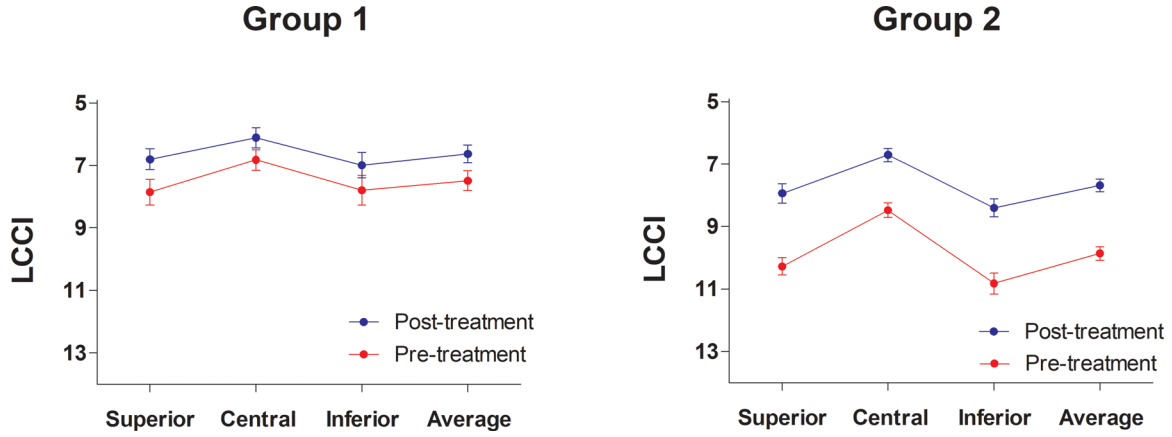

Figure 2. Changes in the LC curvature in response to the IOP reduction in the two NTG groups divided based on the OCT detectable LC curvature change (group 1 (**A**) showed no significant change in LC curvature, whereas group 2 (**B**) showed a significant reversal of LC curvature). Group 2 had larger pretreatment and larger change of the LCCI compared to group 1. LC = lamina cribrosa; IOP = intraocular pressure; NTG = normal tension glaucoma; OCT = optical coherence tomography; LCCI = lamina cribrosa curvature index.

Investigative Ophthalmology & Visual Science

Table 2. Comparative Characteristics of Patients Classified According to the Reversal of LC Curvature

Variables	Group 1 (n = 31) Reversal (−)	Group 2 (n = 62) Reversal (+)	P Value
Baseline clinical characteristics			
Age, years	62.4 ± 9.8	57.6 ± 10.1	0.030
Female gender, n (%)	15 (48.39)	28 (45.16)	0.941
Diabetes mellitus, n (%)	3 (9.68)	7 (11.29)	1.000
Hypertension, n (%)	8 (25.81)	15 (24.19)	1.000
Family history of glaucoma, n (%)	3 (9.68)	4 (6.45)	0.889
Cold extremities, n (%)	7 (22.58)	15 (24.19)	1.000
Migraine, n (%)	3 (9.68)	3 (4.92)	0.669
SBP, mm Hg	122.8 ± 12.4	130.7 ± 12.0	**0.004**
DBP, mm Hg	68.0 ± 9.5	74.4 ± 10.2	**0.005**
MAP, mm Hg	86.3 ± 10.1	93.2 ± 10.4	**0.003**
Baseline ocular characteristics			
IOP, mm Hg	16.3 ± 2.3	15.4 ± 2.5	0.111
Spherical equivalent, diopter	−0.18 ± 1.71	−0.84 ± 2.04	0.127
Central corneal thickness, µm	547.7 ± 36.8	548.2 ± 29.8	0.946
Axial length, mm	23.77 ± 0.82	24.00 ± 1.06	0.301
Global RNFL thickness, µm	79.13 ± 13.48	75.35 ± 16.33	0.270
Visual field MD, dB	−4.25 ± 5.78	−7.07 ± 7.17	0.061
Visual field PSD, dB	4.32 ± 3.31	6.19 ± 4.25	**0.035**
Average BMO width, µm	1416.7 ± 149.7	1387.5 ± 136.2	0.348
Average LCD, µm	**485.1 ± 106.1**	**555.0 ± 138.0**	**0.015**
Average LCCI	**7.49 ± 1.77**	**9.86 ± 1.72**	**<0.001**
Peri-papillary choroidal thickness, µm	145.3 ± 51.6	173.9 ± 62.1	**0.030**
Post IOP lowering treatment			
IOP, mm Hg	11.6 ± 1.7	11.0 ± 1.7	0.082
Reduction of IOP, mm Hg	4.7 ± 1.5	4.5 ± 1.7	0.581
Reduction of IOP (%)	28.51 ± 6.51	28.64 ± 7.40	0.938
Average LCD, µm	**477.5 ± 102.0**	**539.4 ± 135.1**	**0.027**
Reduction of average LCD, µm	**7.8 ± 15.2**	**15.5 ± 20.6**	**0.068**
Average LCCI	**6.70 ± 1.56**	**7.75 ± 1.61**	**0.004**
Reduction of average LCCI	**0.84 ± 0.42**	**2.27 ± 0.58**	**<0.001**

SBP, systolic blood pressure; DBP, diastolic blood pressure; MAP, mean arterial pressure; IOP, intraocular pressure; RNFL, retinal nerve fiber layer; VF, visual field; MD, mean deviation; dB, decibel; PSD, pattern standard deviation; BMO, Bruch's membrane opening; LCD, lamina cribrosa depth; LCCI, lamina cribrosa curvature index.

Data are reported as mean ± standard deviation or n (%).

Table 3. Factors Associated With the Reduction of Lamina Cribrosa Curvature Index in Eyes With LC Reversal (n = 62)

	Univariate Analysis			Multivariate Analysis		
Variables	**Beta**	**95% CI**	**P Value**	**Beta**	**95% CI**	**P Value**
Age, years	**−0.016**	**−0.029 to −0.003**	**0.018**	**−0.014**	**−0.025 to −0.002**	**0.020**
Female gender	−0.048	−0.345 to 0.248	0.745			
Diabetes mellitus	−0.162	−0.629 to 0.305	0.490			
Hypertension	−0.258	−0.590 to 0.075	0.126			
Change of IOP, mm Hg	0.029	−0.060 to 0.118	0.520			
Change of IOP, %	0.014	−0.006 to 0.034	0.157			
Spherical equivalent, D	−0.034	−0.105 to 0.037	0.345			
CCT, µm	−0.003	−0.008 to 0.002	0.224			
AXL, mm	0.082	−0.064 to 0.227	0.267			
Global RNFL thickness, µm	0.006	−0.003 to 0.015	0.158			
Visual field MD, dB	0.014	−0.006 to 0.035	0.171			
Visual field PSD, dB	−0.020	−0.055 to 0.015	0.262			
Average BMO width, µm	0.001	−0.001 to 0.001	0.863			
Baseline LCCI	**0.165**	**0.089 to 0.241**	**<0.001**	**0.158**	**0.085 to 0.232**	**<0.001**

CI, confidence interval; IOP, intraocular pressure; D, diopter; CCT, central corneal thickness; AXL, axial length; RNFL, retinal nerve fiber layer; MD, mean deviation; dB, decibel; PSD, pattern standard deviation; BMO, Bruch's membrane opening; LCCI, lamina cribrosa curvature index.

Statistically significant variables are in boldface.

Only variables with $P < 0.10$ on univariate analysis were included in the multivariate model.

* Stepwise backward regression.

Investigative Ophthalmology & Visual Science

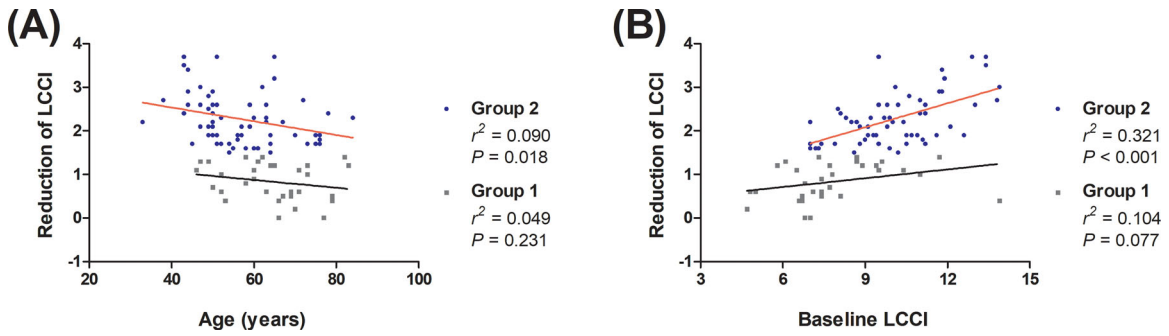

Figure 3. Scatter plots showing the relationships of LCCI reduction with (**A**) baseline age and (**B**) baseline LCCI in the two NTG groups divided based on the OCT detectable LC curvature change (group 1 **A** showed no significant change in LC curvature, whereas group 2 **B** showed a significant reversal of LC curvature). The baseline age and pretreatment LCCI were significantly associated with the change of the LCCI only in the group 2 but not in group 1. LCCI = lamina cribrosa curvature index; NTG = normal tension glaucoma; OCT = optical coherence tomography; LC = lamina cribrosa.

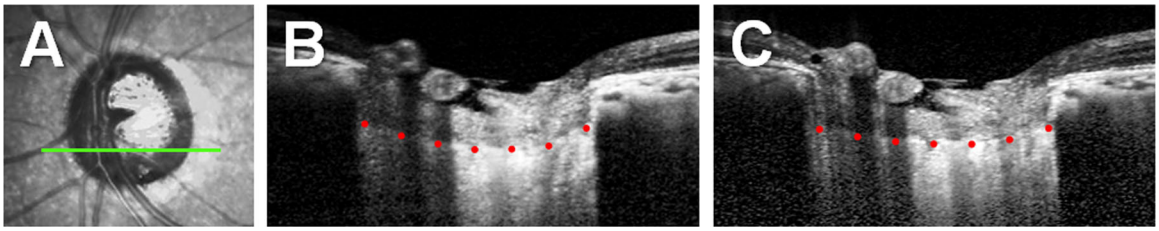

Figure 4. Infrared disc photograph and B-scan images of the left eye of a 60-year-old woman who showed the reversal of LC curvature after lowering IOP from 21 mm Hg to 13 mm Hg. The green line in the infrared disc photograph (**A**) indicates the location of B-scan images at baseline (**B**) and after 1 year of topical IOP-lowering medications (**C**). *Red dots* indicate the anterior surface of the LC. Note that the LC curvature noticeably flattened after IOP lowering treatment. LC = lamina cribrosa; IOP = intraocular pressure.

discrepancy is mainly attributed to the difference in the study subjects. Unlike our previous studies,[31,36] the present study included only patients with NTG. As a result, the magnitude of IOP reduction and the its variation among patients were smaller compared to the previous studies. The smaller range of variation in the two parameters would have made it difficult to detect the correlation between the extent of IOP reduction and the LC curve change.

The baseline LC parameters (LCD and LCCI) predicted the magnititude of LC change in response to the IOP reduction, which is in the line with the results of the study conducted by Quigley et al.[51] It may be presumed that eyes with greater posterior LC deformation are those that are more respondible to IOP change. Together with the absence of correlation between the extent of IOP reduction and the magnitude of LCCI reduction in our study subjects, this finging suggests that the material property of LC plays a central role in the change of LC morphology according to IOP particularly in patients with normal range IOP.

Baseline LCCI in patients with NTG who did not show significant LCCI reduction was 7.73 ± 1.76, similar to that in healthy subjects (7.46 ± 1.22).[30] Interestingly, these patients had a lower systemic BP, a lower OPP, and a thinner peripapillary choroid, vascular factors associated with glaucoma development and/or progression.[46,52,53] These findings suggest that the vascular risk factors may play a more important role in these patients. Glaucoma is regarded as a multifactorial disease, despite elevated IOP being the strongest risk factor for glaucoma. No method has yet been developed to classify patients with glaucoma based on the predominant pathogenic mechanism.

Morphologic changes in the LC were assessed in this study by evaluating LCCI. Although measurement of LC depth from the BMO can be an alternative index, the choroid in glaucomatous eyes becomes thicker after IOP reduction.[54] This may lead to a biased interpretation of changes in LC position from before to after treatment. In contrast, LCCI is not influenced by changes in choroidal thickness. Moreover, it is a simple method that can intuitively indicate the effects of changes in IOP on changes in LC morphology.

Changes in LC morphology may depend on the interval between IOP reduction and OCT imaging. Acute IOP elevation caused by ocular compression did not result in detectable changes in LC morphology, as assessed by measuring LC depth.[55] Therefore, the present study compared LC morphology before and after 1 year of treatment.

The influence of the reversal of LC curvature on glaucoma progression in patients with NTG remains to be elucidated. However, current understanding of the role of LC deformation in the pathogenesis of glaucoma suggests that LC reversal might be a sign of released strain at the level of the LC, providing relief to the compressed RGC axons or lamina capillaries. It would be valuable to assess whether glaucoma is stable or still ongoing in the LCCI reduction group. However, the current study included only patients with consecutive ONH B-scan images before and 1 year after IOP lowering treatment, which were too short to assess the influence of morphologic LC change on disease progression in NTG. Because long-term follow-up data was not available, additional analysis of glaucoma progression in the LCCI reduction group was not possible in the current study.

Further study is needed to evaluate the role of LC reversal in the progression of NTG.

This study had several limitations. First, this study included only a small number of Korean patients, suggesting that there may be a limit to generalize the results of this study and directly applying it to patients of other ethnicities. Second, only the LC within the BMO was included in the measurement of LC curvatures, as the LC outside this region was often not visible. However, the LCCI measured from the entire LC (i.e. between the LC insertions) was comparable to that measured from the LC within the BMO,[31] indicating that the curvature of the LC within the BMO may be a surrogate measurement of the actual LC curvature. Last, because this study did not include the control group (healthy subjects or patients with NTG without IOP change), there may be a limitation to conclude whether the change of LC curvature occurred in the response to IOP reduction in the NTG eyes.

In conclusion, reversal of LC curvature was observed after IOP-lowering treatment in about 60% of patients with NTG. This finding indicates that LC strain plays a central role in optic nerve damage in a large proportion, but not all, patients with NTG.

Acknowledgments

Supported by a grant of Patient-Centered Clinical Research Coordinating Center funded by the Ministry of Health & Welfare, Republic of Korea (grant numbers : HI19C0481 and HC19C0276) and by a grant (06-2021-0017) from the Seoul National University Bundang Hospital Research Fund, Seongnam, Korea. The funding organization had no role in the design or conduct of this research.

Disclosure: **J.A. Kim**, None; **S.H. Lee**, None; **D.H. Son**, None; **T.-W. Kim**, None; **E.J. Lee**, None; **M.J.A. Girard**, None; **J.M. Mari**, None

References

1. Lee SH, Kwak SW, Kang EM, et al. Estimated Trans-Lamina Cribrosa Pressure Differences in Low-Teen and High-Teen Intraocular Pressure Normal Tension Glaucoma: The Korean National Health and Nutrition Examination Survey. *PLoS One*. 2016;11:e0148412.
2. Collaborative Normal-Tension Glaucoma Study Group. Comparison of glaucomatous progression between untreated patients with normal-tension glaucoma and patients with therapeutically reduced intraocular pressures. . *Am J Ophthalmol*. 1998;126:487–497.
3. Yang H, Williams G, Downs JC, et al. Posterior (outward) migration of the lamina cribrosa and early cupping in monkey experimental glaucoma. *Invest Ophthalmol Vis Sci*. 2011;52:7109–7121.
4. Lee KM, Kim TW, Weinreb RN, et al. Anterior lamina cribrosa insertion in primary open-angle glaucoma patients and healthy subjects. *PLoS One*. 2014;9:e114935.
5. Yang H, Ren R, Lockwood H, et al. The Connective Tissue Components of Optic Nerve Head Cupping in Monkey Experimental Glaucoma Part 1: Global Change. *Invest Ophthalmol Vis Sci*. 2015;56:7661–7678.
6. Bellezza AJ, Rintalan CJ, Thompson HW, et al. Deformation of the lamina cribrosa and anterior scleral canal wall in early experimental glaucoma. *Invest Ophthalmol Vis Sci*. 2003;44:623–637.
7. Anderson DR, Hendrickson A. Effect of intraocular pressure on rapid axoplasmic transport in monkey optic nerve. *Invest Ophthalmol*. 1974;13:771–783.
8. Minckler DS, Bunt AH, Johanson GW. Orthograde and retrograde axoplasmic transport during acute ocular hypertension in the monkey. *Invest Ophthalmol Vis Sci*. 1977;16:426–441.
9. Hernandez MR. The optic nerve head in glaucoma: role of astrocytes in tissue remodeling. *Prog Retin Eye Res*. 2000;19:297–321.
10. Burgoyne CF, Downs JC, Bellezza AJ, et al. The optic nerve head as a biomechanical structure: a new paradigm for understanding the role of IOP-related stress and strain in the pathophysiology of glaucomatous optic nerve head damage. *Prog Retin Eye Res*. 2005;24:39–73.
11. Kim JA, Kim TW, Lee EJ, et al. Intereye Comparison of Lamina Cribrosa Curvature in Normal Tension Glaucoma Patients With Unilateral Damage. *Invest Ophthalmol Vis Sci*. 2019;60:2423–2430.
12. Kim GN, Kim JA, Kim MJ, et al. Comparison of Lamina Cribrosa Morphology in Normal Tension Glaucoma and Autosomal-Dominant Optic Atrophy. *Invest Ophthalmol Vis Sci*. 2020;61:9.
13. Kim JA, Lee EJ, Kim TW, et al. Differentiation of Nonarteritic Anterior Ischemic Optic Neuropathy from Normal Tension Glaucoma by Comparison of the Lamina Cribrosa. *Invest Ophthalmol Vis Sci*. 2020;61:21.
14. Kim YW, Lee EJ, Kim TW, et al. Microstructure of beta-zone parapapillary atrophy and rate of retinal nerve fiber layer thinning in primary open-angle glaucoma. *Ophthalmology*. 2014;121:1341–1349.
15. Choi YJ, Lee EJ, Kim BH, Kim TW. Microstructure of the optic disc pit in open-angle glaucoma. *Ophthalmology*. 2014;121:2098–2106.
16. Jonas JB, Papastathopoulos KI. Optic disc shape in glaucoma. *Graefes Arch Clin Exp Ophthalmol*. 1996;234(Suppl 1):S167–S173.
17. Vongphanit J, Mitchell P, Wang JJ. Population prevalence of tilted optic disks and the relationship of this sign to refractive error. *Am J Ophthalmol*. 2002;133:679–685.
18. Samarawickrama C, Mitchell P, Tong L, et al. Myopia-related optic disc and retinal changes in adolescent children from singapore. *Ophthalmology*. 2011;118:2050–2057.
19. Wang YX, Yang H, Luo H, et al. Peripapillary Scleral Bowing Increases with Age and Is Inversely Associated with Peripapillary Choroidal Thickness in Healthy Eyes. *Am J Ophthalmol*. 2020;217:91–103.
20. Rezapour J, Bowd C, Dohleman J, et al. The influence of axial myopia on optic disc characteristics of glaucoma eyes. *Sci Rep*. 2021;11:8854.
21. Spaide RF, Koizumi H, Pozonni MC. Enhanced depth imaging spectral-domain optical coherence tomography. *Am J Ophthalmol*. 2008;146:496–500.
22. Lee EJ, Kim TW, Weinreb RN, et al. Visualization of the lamina cribrosa using enhanced depth imaging spectral-domain optical coherence tomography. *Am J Ophthalmol*. 2011;152:87–95.e1.
23. Girard MJ, Tun TA, Husain R, et al. Lamina cribrosa visibility using optical coherence tomography: comparison of devices and effects of image enhancement techniques. *Invest Ophthalmol Vis Sci*. 2015;56:865–874.
24. Girard MJ, Strouthidis NG, Ethier CR, Mari JM. Shadow removal and contrast enhancement in optical coherence tomography images of the human optic nerve head. *Invest Ophthalmol Vis Sci*. 2011;52:7738–7748.
25. Mari JM, Strouthidis N, Park SC, Girard M. Enhancement of lamina cribrosa visibility in optical coherence tomography images using adaptive compensation. *Invest Ophthalmol Vis Sci*. 2013;54:22382247.
26. Lee SH, Kim TW, Lee EJ, et al. Ocular and Clinical Characteristics Associated with the Extent of Posterior Lamina

Cribrosa Curve in Normal Tension Glaucoma. *Sci Rep*. 2018;8:961.
27. Park SC, Kiumehr S, Teng CC, et al. Horizontal central ridge of the lamina cribrosa and regional differences in laminar insertion in healthy subjects. *Invest Ophthalmol Vis Sci*. 2012;53:1610–1616.
28. Lee EJ, Kim TW, Kim H, et al. Comparison between Lamina Cribrosa Depth and Curvature as a Predictor of Progressive Retinal Nerve Fiber Layer Thinning in Primary Open-Angle Glaucoma. *Ophthalmology Glaucoma*. 2018;1:44–51.
29. Kim JA, Kim TW, Lee EJ, et al. Lamina Cribrosa Morphology in Glaucomatous Eyes with Hemifield Defect in a Korean Population. *Ophthalmology*. 2019;126:692–701.
30. Lee SH, Kim TW, Lee EJ, et al. Lamina Cribrosa Curvature in Healthy Korean Eyes. *Sci Rep*. 2019;9:1756.
31. Lee SH, Yu DA, Kim TW, et al. Reduction of the Lamina Cribrosa Curvature After Trabeculectomy in Glaucoma. *Invest Ophthalmol Vis Sci*. 2016;57:5006–5014.
32. Kim JA, Kim TW, Weinreb RN, et al. Lamina Cribrosa Morphology Predicts Progressive Retinal Nerve Fiber Layer Loss In Eyes with Suspected Glaucoma. *Sci Rep*. 2018;8:738.
33. Lee SH, Kim TW, Lee EJ, et al. Diagnostic Power of Lamina Cribrosa Depth and Curvature in Glaucoma. *Invest Ophthalmol Vis Sci*. 2017;58:755–762.
34. Lee EJ, Kim TW, Kim M, et al. Recent structural alteration of the peripheral lamina cribrosa near the location of disc hemorrhage in glaucoma. *Invest Ophthalmol Vis Sci*. 2014;55:2805–2815.
35. Kiumehr S, Park SC, Syril D, et al. In vivo evaluation of focal lamina cribrosa defects in glaucoma. *Arch Ophthalmol*. 2012;130:552–559.
36. Lee EJ, Kim TW, Weinreb RN. Reversal of lamina cribrosa displacement and thickness after trabeculectomy in glaucoma. *Ophthalmology*. 2012;119:1359–1366.
37. Spaide RF, Koizumi H, Pozzoni MC. Enhanced depth imaging spectral-domain optical coherence tomography. *Am J Ophthalmol*. 2008;146:496–500.
38. Li L, Bian A, Zhou Q, Mao J. Peripapillary choroidal thickness in both eyes of glaucoma patients with unilateral visual field loss. *Am J Ophthalmol*. 2013;156:1277–1284.e1.
39. Benjamini Y, Hochberg Y. Controlling the false discovery rate: a practical and powerful approach to multiple testing. *J R Stat Soc. B Method*. 1995;57:289–300.
40. Jampel HD, Vitale S, Ding Y, et al. Test-retest variability in structural and functional parameters of glaucoma damage in the glaucoma imaging longitudinal study. *J Glaucoma*. 2006;15:152–157.
41. Quigley HA. The pathogenesis of reversible cupping in congenital glaucoma. *Am J Ophthalmol*. 1977;84:358–370.
42. Ogden TE, Duggan J, Danley K, et al. Morphometry of nerve fiber bundle pores in the optic nerve head of the human. *Exp Eye Res*. 1988;46:559–568.
43. Albon J, Karwatowski WS, Easty DL, et al. Age related changes in the non-collagenous components of the extracellular matrix of the human lamina cribrosa. *Br J Ophthalmol*. 2000;84:311–317.
44. Prata TS, De Moraes CG, Teng CC, et al. Factors affecting rates of visual field progression in glaucoma patients with optic disc hemorrhage. *Ophthalmology*. 2010;117:24–29.
45. Nouri-Mahdavi K, Hoffman D, Coleman AL, et al. Predictive factors for glaucomatous visual field progression in the Advanced Glaucoma Intervention Study. *Ophthalmology*. 2004;111:1627–1635.
46. Leske MC, Heijl A, Hyman L, et al. Predictors of long-term progression in the early manifest glaucoma trial. *Ophthalmology*. 2007;114:1965–1972.
47. Fazio MA, Grytz R, Morris JS, et al. Age-related changes in human peripapillary scleral strain. *Biomech Model Mechanobiol*. 2014;13:551–563.
48. Grytz R, Fazio MA, Libertiaux V, et al. Age- and race-related differences in human scleral material properties. *Invest Ophthalmol Vis Sci*. 2014;55:8163–8172.
49. Fazio MA, Grytz R, Morris JS, et al. Human scleral structural stiffness increases more rapidly with age in donors of African descent compared to donors of European descent. *Invest Ophthalmol Vis Sci*. 2014;55:7189–7198.
50. Yang H, He L, Gardiner SK, et al. Age-related differences in longitudinal structural change by spectral-domain optical coherence tomography in early experimental glaucoma. *Invest Ophthalmol Vis Sci*. 2014;55:6409–6420.
51. Quigley H, Arora K, Idrees S, et al. Biomechanical Responses of Lamina Cribrosa to Intraocular Pressure Change Assessed by Optical Coherence Tomography in Glaucoma Eyes. *Invest Ophthalmol Vis Sci*. 2017;58:2566–2577.
52. Kwon J, Jo YH, Jeong D, et al. Baseline Systolic versus Diastolic Blood Pressure Dip and Subsequent Visual Field Progression in Normal-Tension Glaucoma. *Ophthalmology*. 2019;126:967–979.
53. Lee KM, Lee EJ, Kim TW. Juxtapapillary choroid is thinner in normal-tension glaucoma than in healthy eyes. *Acta Ophthalmol*. 2016;94:e697–e708.
54. Vianna JR, Lanoe VR, Quach J, et al. Serial Changes in Lamina Cribrosa Depth and Neuroretinal Parameters in Glaucoma: Impact of Choroidal Thickness. *Ophthalmology*. 2017;124:1392–1402.
55. Agoumi Y, Sharpe GP, Hutchison DM, et al. Laminar and prelaminar tissue displacement during intraocular pressure elevation in glaucoma patients and healthy controls. *Ophthalmology*. 2011;118:52–59.

Investigative Ophthalmology & Visual Science